Agricultural and Forest Meteorology 333 (2023) 109398

Contents lists available at ScienceDirect

Agricultural and Forest Meteorology

journal homepage: www.elsevier.com/locate/agrformet

The effect of tree decline over soil water content largely controls soil respiration dynamics in a Mediterranean woodland

Alexandra Rodríguez [a,b,*,1], Jorge Durán [a,b], Jorge Curiel Yuste [c,d], Fernando Valladares [e,f,g], Ana Rey [e]

[a] Centre for Functional Ecology, CFE, University of Coimbra, 3000-456 Coimbra, Portugal
[b] Misión Biolóxica de Galicia, Consejo Superior de Investigaciones Científicas, 36143 Pontevedra, Spain
[c] BC3 - Basque Centre for Climate Change, Scientific Campus of the University of the Basque Country, 48940 Leioa, Spain
[d] IKERBASQUE - Basque Foundation for Science, Maria Diaz de Haro 3, 6 solairua, 48013 Bilbao, Bizkaia, Spain
[e] Department of Biogeography and Global Change, National Museum of Natural Sciences, MNCN, CSIC, 28006 Madrid, Spain
[f] LINCGlobal, Madrid, Spain
[g] Area of Biodiversity and Conservation, ESCET, Rey Juan Carlos University, 28933 Móstoles, Madrid, Spain

ARTICLE INFO

Keywords:
Quercus ilex
Forest die-off
Climate change
Soil functioning
Soil CO_2 efflux
Environmental control

ABSTRACT

As drought-induced tree defoliation and mortality (i.e. tree decline) in the Mediterranean is expected to worsen with ongoing climate change, it is of paramount importance to understand how, why, and when tree decline affects soil respiration (R_s). We carried out a novel study exploring the interacting effects of climatic variability (i.e. season and year) and tree decline on soil water content (SWC), soil temperature (T_{soil}), and R_s temporal variability in a Mediterranean holm oak woodland. The study further explores the effects of tree decline on the main controls of R_s at the stand scale (i.e. plant variables, SWC, T_{soil}, and soil physicochemical variables). We monitored R_s, T_{soil}, and SWC under the canopy of 30 holm oak trees with different defoliation degrees (healthy, affected, and dead) during two years of contrasting precipitation patterns. We estimated different plant structural variables (e.g. height, canopy diameter) on those selected trees under whose canopies we also collected soil samples to analyze different soil physicochemical variables. Our study provides, up to our knowledge, the first observational (i.e. in situ) evidence that tree decline might decrease the positive response of R_s to increased precipitation and drying-rewetting cycles. It also suggests that tree decline can significantly increase SWC and decrease R_s but largely depending on the declining stage, the year, and the season. Finally, tree decline affected the relative importance of the different drivers of R_s, with both SWC and T_{soil} gaining importance as trees defoliate and die. Altogether, our results point towards a negative impact of drought-induced tree decline on soil carbon (C) content and cycling, particularly under forecasted climate change scenarios with dryer and more intense precipitation regimes.

1. Introduction

Climate models in Mediterranean ecosystems forecast increases in temperature and more intensive and extensive droughts, with more frequent and intense extreme temperature and precipitation events (IPCC, 2021). These changes will affect the structure, composition, and functioning of forests in still unknown ways, with important implications for the C balance (Liu et al., 2016; Reichstein et al., 2013; Wang et al., 2012). Forecasted changes in the frequency, intensity, and distribution of rainfall events (IPCC, 2021) will likely increase the importance of rainfall pulses on the C cycle of Mediterranean environments (Liu et al., 2016; Rey et al., 2021, 2017; Rousk and C. Brangarí, 2022; Wang et al., 2016), largely influenced by the intra-annual variation in soil water content (Gallardo et al., 2009). Also, the increasingly dry and hot climatic conditions will exacerbate the drought-induced tree defoliation and mortality (hereinafter "forest die-off") observed over the past two decades (Carnicer et al., 2011; Lloret et al., 2004).

Drought-induced forest die-off impacts forest ecosystems by reducing tree productivity, reducing the input of litter and root exudates, and modifying soil microclimatic conditions, and in turn, soil

* Corresponding author.
E-mail address: alexandra.rodriguez@csic.es (A. Rodríguez).
[1] Present postal address of the corresponding author: Misión Biolóxica de Galicia, Consejo Superior de Investigaciones Científicas, 36143 Pontevedra, Spain.

https://doi.org/10.1016/j.agrformet.2023.109398
Received 14 October 2022; Received in revised form 24 February 2023; Accepted 26 February 2023
Available online 10 March 2023

microbial communities (Schlesinger et al., 2016). Accordingly, Rodríguez et al. (2017, 2020) found evidence of a cascade effect of ongoing drought-induced forest die-off in a Mediterranean holm oak (*Quercus ilex*) woodland ultimately decreasing the content and lability of soil C. Although efforts to understand the effects of forest die-off on important soil processes related to C cycling have increased lately (Avila et al., 2019, 2016; Curiel Yuste et al., 2019; García-Angulo et al., 2020), results are still scarce and contradictory. For instance, some studies have reported decreases in R_s as a result of reduced root activity (Avila et al., 2016), whereas others have found no changes (Barba et al., 2016) or even increased rates (Barba et al., 2013; Curiel Yuste et al., 2019; Edburg et al., 2012) following increases in soil moisture, litter inputs, and secondary successional processes. Thus, the impacts of forest die-off on R_s are complex and largely depend on the balance of its effects on roots (autotrophic) and microbial (heterotrophic) components (Avila et al., 2016). Moreover, recent studies suggest that forest die-off can largely modulate the response of microbial respiration to climate change and that forest die-off effects on different soil biogeochemical conditions and processes are seasonal due to changes in biotic activity (Avila et al., 2019, 2016; Rodríguez et al., 2019). Still, the interacting effects of tree decline and climatic variability (i.e. season and year) on R_s have been scarcely explored, specifically in the field and considering Mediterranean forests and drought as the main driver of tree decline (Barba et al., 2016).

Soil respiration is the largest source of CO_2 from terrestrial ecosystems and, therefore, a central piece of the global C balance (Schlesinger and Andrews, 2000). However, it is also a very complex process controlled by several physiological, phenological, and environmental processes that vary both in time and space (Rey et al., 2021, 2011; Tang and Baldocchi, 2005). At the global scale, its temporal and spatial variability is mainly controlled by air temperature and precipitation, whereas at micro and stand scales, other factors related to plant community and soil organic matter become more important (Barba et al., 2013; Raich and Schlesinger, 1992). Moreover, whereas autotrophic respiration (R_A) is mainly controlled by tree physiology and productivity (Högberg et al., 2001; Matteucci et al., 2015), heterotrophic respiration (R_H) is largely controlled by soil water content and temperature and biogeochemical factors (e.g. organic matter content and quality, microbial community structure) (Curiel Yuste et al., 2007; Tang and Baldocchi, 2005; Zhao et al., 2016). This complexity is at least partially responsible for the large uncertainties associated with predictions of global rates of R_s and R_s responses to climate change (Warner et al., 2019). Thus, there is an urgent need to continue to study this critical ecosystem process under different scenarios and at different temporal and spatial scales.

Our main aim is to help advance the mechanistic understanding of the effects of tree decline on the R_s of Mediterranean forests and its relationship with SWC, T_{soil}, and other potential controls. To do so, we specifically explored i) the interacting effects of season and year and different stages of tree decline (i.e. healthy, affected, and dead) on SWC, T_{soil}, and R_s in a *Quercus ilex* Mediterranean woodland and ii) the effects of tree decline on the main controls of R_s at the stand scale (i.e. plant variables and soil microclimatic and physicochemical variables). We hypothesized that i) tree decline modifies soil microclimatic conditions, particularly SWC, and, in turn, R_s rates and that ii) these effects would vary among seasons and years due to contrasting biotic activity and precipitation conditions (i.e. amount and distribution), respectively. Moreover, assuming changes in the relative contribution of R_A and R_H associated with the tree decline (Curiel Yuste et al., 2019), we hypothesized that iii) the relative importance of SWC and T_{soil} and physicochemical variables controlling R_s would increase against that of plant variables from considering the whole decline gradient (i.e. grouping healthy, affected and dead trees) to considering each stage separately in increasing decline.

2. Material and methods

2.1. Study site

The study was carried out in a holm oak woodland located in the central part of the Iberian Peninsula, southwest of Madrid (40°23′N, 4°11′W; 630–660 m above sea level). The climate is continental Mediterranean with a mean annual temperature of 15 °C (Winter: 8 °C; Spring: 16 °C; Summer: 23 °C; Autumn: 11 °C) and mean annual precipitation of 558 mm (Winter: 160 mm; Spring: 131 mm; Summer: 57 mm; Autumn: 214 mm) (Ninyerola et al., 2005). Most rainfall concentrates from autumn to spring, while summers are warm and dry. Soil is a Cambisol, sandy and slightly acid (pH~6.3), with low total C (~1.9%) and nitrogen (N; ~0.15%) content (Rodríguez et al., 2017; Table S1). Aboveground vegetation is characterized by a tree density of ~180 trees ha^{-1}, mostly composed of *Quercus ilex* L. ssp. *ballota* [Desf.] Samp (holm oak) with scarce *Juniperus oxycedrus* Sibth. & Sm (cedar). The understory is dominated by *Retama sphaerocarpa* L., *Lavandula stoechas* ssp. *pedunculata* (Mill.) Samp. ex Rozeira, and diverse pasture species (Rodríguez et al., 2017). In 2005, this region suffered a strong event of holm oak defoliation (around 20–30% of the total population) and mortality (15%) due to a severe drought. Since then, the holm oaks of this woodland have shown different decline stages (healthy, affected, and dead) with contrasting soil physicochemical conditions underneath such as inorganic N concentrations and labile C (Rodríguez et al., 2020, 2017; Table S1).

2.2. Experimental design

In spring 2013, we selected 30 holm oak adult trees of similar size (38 cm and 4 m of diameter at breast height and height on average, respectively, Table S1) but with different levels of canopy decline (10 healthy, 10 affected, and 10 dead), and consequently with significantly different canopy diameter (Table S1; Rodríguez et al., 2017), separated at least 10 m from other trees. The canopy decline status of the different trees was visually determined – *healthy* (< 10% defoliated); *affected* (> 50% defoliated); *dead* (100% defoliated).

For each tree, we established a sampling point below the influence of the tree canopy, 0.3 m away from the trunk (Rodríguez et al., 2017). All sampling points were established at the north face of the trunk to avoid confounding factors due to orientation. Polyvinylchloride soil collars (15 cm in diameter and 7 cm in height) were inserted 3.5 cm into the soil at each sampling point one week before we took the first R_s measurements, where they remained for two consecutive annual periods: from June 2013 to May 2014 (*year 1*) and from June 2014 to May 2015 (*year 2*).

Both annual periods were extremely warm according to the reference period (1971–2000 and 1981–2010 until and from January 2015, respectively; AEMET), with similar mean annual air temperatures (15.9 °C and 15.8 °C, respectively) but lower precipitation values in *year 1* (288.8 mm) than in *year 2* (343.3 mm), particularly in late summer and fall (Fig. 1).

2.3. Soil microclimate and soil respiration measurements

We monitored R_s, along with T_{soil} and SWC, in all sampling points from June 2013 to May 2015 at a frequency of approximately twice a month during spring and fall and once a month during summer and winter (30 campaigns in total; Fig. 1). To avoid strong diurnal fluctuations, measurements were done during the midday period (between 10:00 and 14:00 h). Moreover, special care was taken to fully randomize the sampling sequence across tree decline stages in each measurement campaign. Small plants, excessive litter, insects, and grasses were carefully removed from each collar before each R_s measurement. A portable infrared gas analyzer (IRGA) connected to a soil respiration chamber (EGM-4 and SRC-1; PP Systems, USA) was used to measure R_s

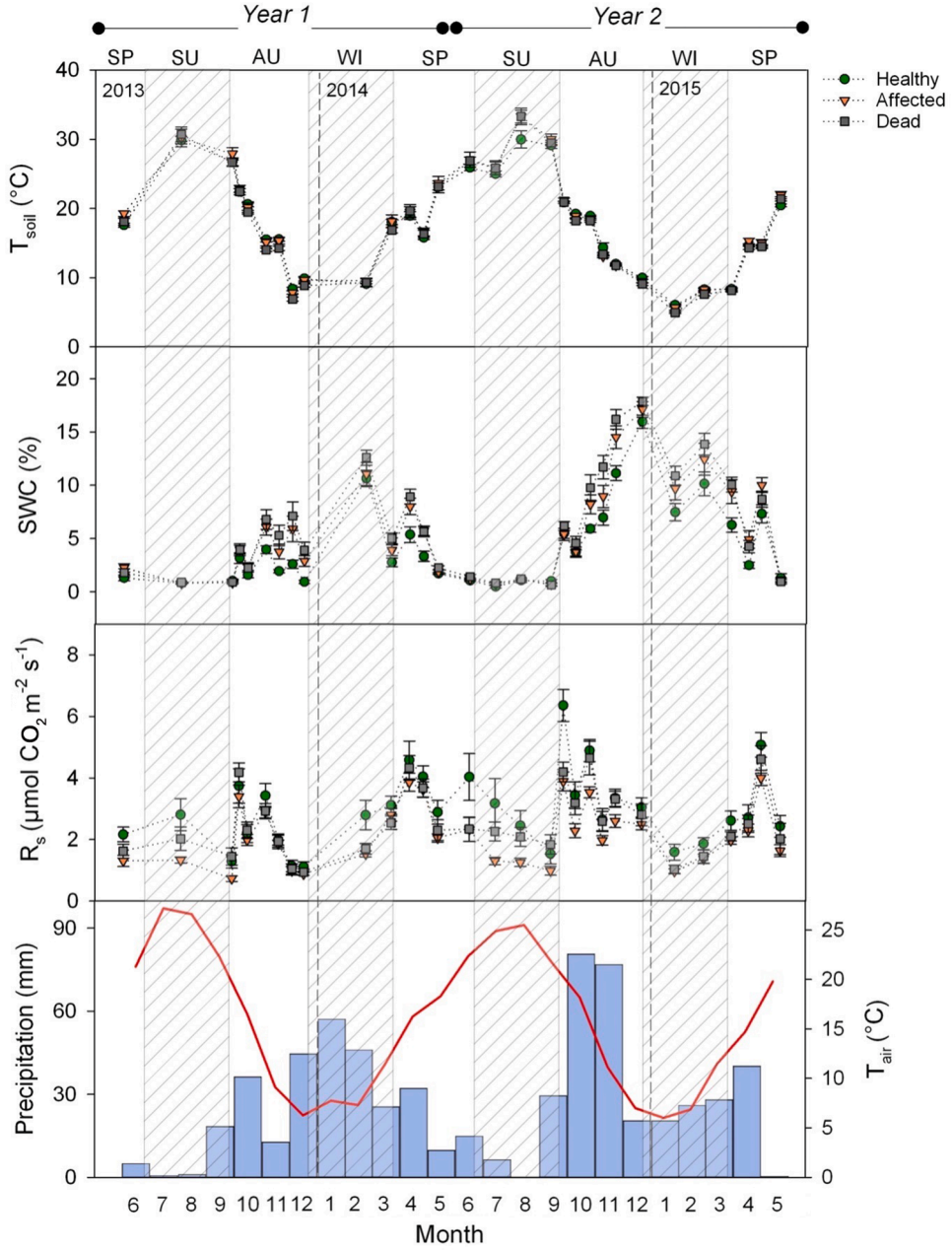

Fig. 1. Temporal dynamics of soil temperature (T_{soil}), soil volumetric water content (SWC), and soil respiration (R_s) measured under the canopy of each tree decline stage (healthy, affected and dead), as well as the precipitation and air temperature (T_{air}) spanning the study period (June 2013 – May 2015). Dots and error bars represent the mean ± 1 SE (n = 10). SP = Spring; SU = Summer; AU = Autumn; WI = Winter.

rates (g CO_2 m^{-2} h^{-1}) in situ. Linear increase of CO_2 concentration within the chamber was measured for 90 s with measurements every 4 s ensuring reliable estimations. We further added to the chamber volume of the commercial chamber (1171 cm3) the extra volume generated from the collars and expressed R_s both by µmol CO_2 m^{-2} s^{-1} (1 mol CO_2 = 44.009 g) and on a C basis (µmol CO_2 kg C^{-1} s^{-1}) using the soil bulk density in each sampling point. At the time of each R_s measurement, two measurements of T_{soil} and SWC were also carried out on confronted sides of the collar and close to it at 4 cm depth (the most active) inserting vertically a soil digital thermometer (Maxtech, Lokhnath Enterprise, India) and a time-domain reflectometer (Fieldscout TDR 300, Spectrum Technologies, Inc., Plainfield, IL, USA), respectively. The two measurements of T_{soil} and SWC were averaged to obtain just one value per sampling point and time.

We estimated seasonal (spring, summer, fall, and winter of *year 1* and *year 2*), annual (*year 1* and *year 2*), and two-year (the whole study period) average values of R_s, T_{soil}, and SWC for each sampling point considering all the temporal measures carried out within each respective period. Whereas our experimental design hardly provides accurate daily, seasonal, or annual R_s estimations, it is perfectly valid in terms of comparison among the different decline stages and correlations with the different predictor variables.

2.4. Plant and soil physicochemical variables

At the end of May 2013, we measured tree height, diameter at breast height (DBH), and the canopy diameter of the 30 studied trees by using a clinometer, a DBH tape, and averaging two perpendicular measurements of canopy diameter, respectively. We also estimated a distance-dependent competition index between trees for each one of the

studied trees (Hegyi, 1974), considering all the competing holm oaks and cedars within a 5.5 m radius, the DBH of the subject tree and that of its competitors as well as the distance between the subject tree and its competitors (Table S1; Rodríguez et al., 2017). On the same date, we also measured soil compaction in all sampling points by using a soil compaction meter (FieldScout SC 900, USA).

We carried out two different soil samplings in May 2013 (start of the study) and March 2015 (end of the study) to estimate various physico-chemical variables (i.e. total C and N, pH, labile C, bulk density) for each decline stage (healthy, affected, and dead). Soil samples were collected close to the soil collars and from the first 10 cm of the soil profile by using a 5 cm (inside diameter) metal corer and then kept at 4 °C until analysis. Before analysis, soil samples were sieved (2 mm mesh size), homogenized in field-moist conditions, and analyzed for gravimetric moisture by oven-drying a subsample at 60 °C to constant mass. Soil total C and N content, and soil pH, were analyzed in soil samples collected in May 2013 by dry combustion with an elemental analyzer (LECO TruSpec CN, St. Joseph, MI, USA) and using a soil-to-water ratio of 1:2.5 (m/v), respectively. The possible occurrence of inorganic C was checked by a Dietrich-Fruhling volumetric calcimeter. Given its absence, total C was considered equal to soil organic C. Labile C was determined in the 2015 samples by using the High Gradient Magnetic Separation (HGMS) method as described in Rodríguez et al. (2020). Briefly, 10 gs of each sample underwent HGMS by a Frantz Isodynamic Separator (Model L-1, SG Frantz Co, Inc., Trenton, New Jersey, USA) that separated each soil sample in two fractions with different turnover times, a non-magnetic and a magnetic fraction (Chiti et al., 2019). The magnetic fraction (MA) has larger contributions from relatively recent C forms than the non-magnetic fraction and thus, is supposed to be more labile. We analyzed total C in the MA fraction (C_{MA}) by dry combustion (see above) and considered it as labile C. Soil bulk density was also estimated in the soil samples collected in 2015 (Table S1).

2.5. Statistical analyses

Linear models were performed to relate seasonal air temperature and precipitation values with our estimated T_{soil} and SWC seasonal values, respectively, as indicative of the suitability of our seasonal measurements.

We used generalized least squares (GLS) models to test the effects of year, season, and tree decline status, as well as their interactions, on SWC, T_{soil}, and R_s. Pairwise statistical differences among the means of the factor levels were tested using simultaneous tests for general linear hypotheses (multiple comparisons of means: Tukey contrasts). For all the GLS models, the tree was used as a random factor to account for temporal dependencies and, when necessary, no-normality and heteroscedasticity of the residuals were corrected by log-transforming the dependent variable and/or using the argument weights, respectively.

We explored the relationship between R_s and T_{soil} for the whole sampling period and each decline stage separately using averaged values for each temperature degree. We identified two different periods visually determined by a temperature threshold from which the relationship of R_s with T_{soil} changes (Period I – below the temperature threshold, most of the year except summer; and Period II –from the threshold, summer) (Figure S1). For Period I, soil respiration was considered dependent on soil temperature according to an exponential relationship:

$$R_s = R_{basal} * e^{b*T} \quad (1)$$

where R_s is the soil respiration (μmol CO_2 m^{-2} s^{-1}), T is soil temperature (°C) measured at a depth of 4 cm, and R_{basal} (the basal respiration rate) and b are fitted parameters. The Q_{10} (the increase in R_s for a 10 °C increase in temperature) was calculated as follows:

$$Q_{10} = e^{10*b} \quad (2)$$

For Period II, R_s was better explained by soil water content through a logarithmic function:

$$R_s = a + b * ln(SWC) \quad (3)$$

where SWC (%) is soil volumetric water content measured at the depth of 4 cm, and a and b are fitted parameters.

We then used a multimodel inference approach based on information theory and ordinary least-squares (OLS) regressions to evaluate the relative importance of plant (canopy diameter) and soil microclimatic (two-year average values of T_{soil} and SWC) and physicochemical (C_{MA}, total N, bulk density) variables on the two-year average values of R_s for all decline stages together and separately (Burnham and Anderson, 2010). These variables were selected based on their ecological importance to the ecosystem functioning (Guerra et al., 2022), their relationship with R_s, and their independence from each other (Figure S2, supplementary material). Canopy diameter was shown to be significantly affected by tree defoliation degree (Table S1; Rodríguez et al., 2017) and thus considered as a surrogate of tree decline status ($R^2_{adj} = 0.30$, $P < 0.01$).

We used R 3.6.1 (R Core Team, 2017) for GLS models (nlme; Pinheiro et al., 2020), multiple comparisons between the means of the factor levels (multicomp; Bretz et al., 2011) and spearman correlations between our different variables (corrplot; Taiyun and Simko, 2017). Also, we used SigmaPlot 14.0 (Systat Software, San Jose, CA) to study the relationship of R_s with T_{soil} and SWC, and SAM 4.0 (Rangel et al., 2010) for the multimodel inference approach.

3. Results

Similar to air temperature and precipitation, T_{soil} and SWC showed large and opposed ($\rho = -0.70$, $P < 0.001$) seasonal dynamics typical of the Mediterranean climate (Fig. 1; Table S2). Despite the limited and irregular number of T_{soil} and SWC measurements per season and year, our estimated seasonal values for these two soil microclimatic variables were largely explained by seasonal air temperature (75%) and precipitation (87%), respectively ($P < 0.001$) (Table S2).

3.1. Interacting effects of year, season, and tree decline on soil microclimate and r_s

Both years showed similar annual means (18 °C and 17.7 °C, respectively) and seasonal dynamics (Fig. 1; Table 1 and S2) of T_{soil}. On the contrary, annual means of SWC were significantly lower (43%) in *year 1* than in *year 2* (Table 1), and whereas the minimum SWC values of both years occurred in mid-summer (~ 0.1%), maximum values were found in winter for *year 1* (15%) and in autumn for *year 2* (22%; Fig. 1, Table S2). Similarly, R_s was significantly lower in *year 1* than in *year 2* (2.37 vs. 2.72 μmol CO_2 m^{-2} s^{-1}, respectively; Table 1) and showed a significant interaction between year and season tightly linked to the different seasonal dynamics (intra-annual variability) of SWC for both years (Table S2). Thus, while in *year 1*, R_s picked in spring and showed the lowest values in fall, in *year 2*, R_s peaked in fall and showed the lowest values in winter (Fig. 1, Table S2). Consequently, seasonal means of R_s were 68% lower in *fall 1* than in *fall 2*, but 70% higher in *winter 1* than in *winter 2* (Table S2). The above-described differences in SWC between years and among seasons were independent of the defoliation degree. However, in the case of R_s, we found a significant interaction between decline status and year with annual means significantly higher (22%) in *year 2* than in *year 1* under healthy but not under affected (5%) and dead (16%) trees (Table 1).

Considering the whole studied period, T_{soil} ranged between 5–34 °C, 4–37 °C, and 5–41 °C under healthy, affected, and dead trees, respectively, with similar average values (~18 °C) under all decline stages. Thus, although the maximum T_{soil} values increased with defoliation degree, we found neither a significant overall effect of tree decline nor a significant interaction between decline status and year on T_{soil} (Table 1).

Table 1
Annual means of soil water content (SWC), soil temperature (T_{soil}), and soil respiration (R_s) for the two studied years, from June 2013 to May 2014 (*year 1*) and from June 2014 to May 2015 (*year 2*) ($n = 10$ in all cases). Values represent the mean ± 1SE. Bold *P* values represent statistically significant effects of tree decline (*De*) and year (*Y*), as well as significant interactions of both factors found through the chi-squared test (χ^2). Values with different letters within each year represent significant differences among decline stages (healthy, affected, and dead) and underlined values denote a significant year effect for the respective decline stage ($P < 0.05$).

Variable	Year	Decline stage			GLS models		
		Healthy	Affected	Dead		χ^2	*P*
SWC (%)	*year 1*	2.9 ± 0.2b	4.3 ± 0.4ab	4.8 ± 0.4a	*De*	14.8	**<0.001**
	year 2	5.5 ± 0.3b	6.8 ± 0.5ab	7.4 ± 0.4a	*Y*	362.8	**<0.001**
					De x Y	0.58	0.749
T_{soil} (°C)	*year 1*	18.0 ± 0.2	18.3 ± 0.5	17.6 ± 0.3	*De*	1.27	0.529
	year 2	17.6 ± 0.2	18.0 ± 0.4	17.6 ± 0.3	*Y*	3.52	0.060
					De x Y	2.41	0.300
R_s (μmol CO_2 m^{-2} s^{-1})	*year 1*	2.66 ± 0.25	2.09 ± 0.08	2.35 ± 0.22	*De*	2.48	0.289
	year 2	3.24 ± 0.34a	2.19 ± 0.09b	2.72 ± 0.25ab	*Y*	19.1	**<0.001**
					De x Y	14.0	**<0.001**
R_s (μmol CO_2 kg C^{-1} s^{-1})	*year 1*	1.04 ± 0.10	0.91 ± 0.09	0.90 ± 0.11	*De*	2.62	0.270
	year 2	1.26 ± 0.13	0.94 ± 0.08	1.07 ± 0.12	*Y*	42.5	**<0.001**
					De x Y	17.5	**<0.001**

However, we did find a significant interaction between decline status and season on T_{soil} of *year 2*, with significantly higher values under healthy than under dead trees in fall (Table 2). In the case of SWC, tree decline had a significant overall and positive effect, with significantly higher SWC values under dead (6.1% on average) than under healthy (4.3%) trees, and intermediate values under affected (5.6%; Table 1) trees. These differences were independent of the year but not of the seasonality, as neither *winter 2* nor any of the summers showed those differences among decline stages (Table 2). Finally, considering the whole studied period, R_s ranged between 0.39–9.22, 0.07–6.02, and 0–7.51 μmol CO_2 m^{-2} s^{-1} under healthy, affected, and dead trees, with average values of 2.96, 2.14, and 2.54 μmol CO_2 m^{-2} s^{-1} respectively. Although we did not find a significant overall effect of tree decline on R_s, we did find a significant interaction between decline status and year, with values 48% and 19% higher under healthy than under affected and dead trees, respectively, in *year 2* ($P < 0.001$; Table 1). These differences were observed in all seasons, except in spring (Table 2). Moreover, in *year 1* we found a significant interaction between decline status and season, with R_s values in summer and winter up to 111% higher under healthy than under declining trees (Table 2). When expressing R_s on a C basis (i.e. per unit of soil organic C), we also obtained a significant interaction between decline status and year with a trend to lower values under affected (14% and 33% for years *1* and *2*, respectively) and dead (15% and 17% for year 1 and 2, respectively) than under healthy trees but without significant differences among decline stages (Table 1).

3.2. Tree decline modulates the relationship between R_s and soil microclimatic variables

Based on the above-discussed differences found among tree decline stages, R_s was modeled as a function of T_{soil} and SWC for each decline stage separately. Moreover, as explained in the Methods section, we identified two different periods determined by a T_{soil} threshold (17 °C for healthy and dead and 18 °C for affected trees), below (Period I) and above (Period II) which R_s was considered dependent on T_{soil} and SWC, respectively (Fig. S1, Supplementary material). Those temperature thresholds corresponded to SWC values of 4%, 5%, and 7% for healthy, affected, and dead trees, respectively. Period I mostly corresponded to

Table 2
Seasonal means of soil water content (SWC), soil temperature (T_{soil}), and soil respiration (R_s) for the two studied years and all tree decline stages separately ($n = 10$ in all cases). Values represent the mean ± 1SE. Bold *P* values represent statistically significant effects of the season (S), as well as significant tree decline x season (De x S) interactions found through the chi-squared test (χ^2). Values with different capital letters within each year and season represent significant differences among tree decline stages. Values with different lowercase letters within each year and tree decline stage represent significant differences among seasons ($P < 0.05$).

	Decline stage			GLS models		
	Healthy	Affected	Dead		χ^2	*P*
			SWC (%)			
year 1						
Summer	0.8 ± 0.1c	0.8 ± 0.1c	0.9 ± 0.1c	De	0.54	0.763
Fall	2.2 ± 0.2Bb	3.7 ± 0.5Ab	4.3 ± 0.6Ab	S	505.3	**<0.001**
Winter	6.7 ± 0.5Ba	7.5 ± 0.7ABa	8.8 ± 0.5Aa	De x S	42.1	**<0.001**
Spring	2.9 ± 0.3Bb	4.5 ± 0.3Ab	4.7 ± 0.3Ab			
year 2						
Summer	0.9 ± 0.1c	0.9 ± 0.1c	0.9 ± 0.1c	De	14.4	**<0.001**
Fall	8.2 ± 0.4Ba	9.7 ± 0.6ABa	11.1 ± 0.7Aa	S	2295.5	**<0.001**
Winter	9.4 ± 1.0a	11.3 ± 1.2a	12.9 ± 1.0a	De x S	6.36	0.384
Spring	3.7 ± 0.4Bb	5.3 ± 0.4Ab	5.0 ± 0.3Ab			
			T_{soil} (°C)			
year 1						
Summer	29.9 ± 0.5a	30.2 ± 1.3a	30.7 ± 1.0a	De	7.72	< 0.05
Fall	17.0 ± 0.2c	17.0 ± 0.4c	16.1 ± 0.2c	S	1351.0	**<0.001**
Winter	13.6 ± 0.3d	13.8 ± 0.6d	13.1 ± 0.4d	De x S	8.08	0.232
Spring	18.9 ± 0.3b	19.8 ± 0.6b	19.3 ± 0.5b			
year 2						
Summer	28.0 ± 0.4a	29.7 ± 0.8a	29.5 ± 0.6a	De	3.21	0.201
Fall	15.9 ± 0.1Ab	15.6 ± 0.3ABc	15.3 ± 0.2Bc	S	9630.6	**<0.001**
Winter	7.5 ± 0.2c	7.3 ± 0.3d	6.7 ± 0.4d	De x S	29.7	**<0.001**
Spring	16.8 ± 0.1b	17.5 ± 0.5b	17.1 ± 0.3b			
			R_s (μmol CO_2 m^{-2} s^{-1})			
year 1						
Summer	2.80 ± 0.52Aab	1.33 ± 0.10Bc	2.02 ± 0.38ABb	De	1.69	0.429
Fall	2.12 ± 0.24b	1.82 ± 0.10bc	2.11 ± 0.21b	S	68.6	**<0.001**
Winter	2.95 ± 0.33Aa	2.17 ± 0.12ABb	2.12 ± 0.19Bb	De x S	25.9	**<0.001**
Spring	3.24 ± 0.34a	2.71 ± 0.13a	2.98 ± 0.28a			
year 2						
Summer	2.38 ± 0.51Ab	1.18 ± 0.09Bb	2.06 ± 0.28ABb	De	16.0	< 0.001
Fall	3.95 ± 0.33Aa	2.79 ± 0.14Ba	3.46 ± 0.30ABa	S	180.6	**<0.001**
Winter	1.77 ± 0.18Abc	1.15 ± 0.08Bb	1.28 ± 0.15Bc	De x S	13.8	**< 0.05**
Spring	3.37 0.39a	2.44 ± 0.12a	2.76 ± 0.29ab			

fall, winter, and spring microclimatic conditions, whereas Period II mostly corresponded to summer conditions.

During Period I, R_s related to T_{soil} through an exponential relationship that explained the 72%, 91%, and 75% of the variance for healthy, affected, and dead trees, respectively, and with values of estimated basal respiration of 1.053 (SE 0.221), 0.662 (SE 0.089) and 0.832 (SE 0.177) μmol CO_2 m^{-2} s^{-1}, and Q_{10} values of 2.16, 2.48 and 2.32 (Fig 2a, b, and c). During Period II, R_s was related to SWC through a logarithmic function, explaining 18%, 69%, and 56% of the variance for healthy, affected, and dead trees, respectively (Fig 2d, e, and f). These results point out tree decline status as a modulator of the relationship of R_s with soil microclimatic variables, particularly with SWC, suggesting a higher control of R_s by SWC under affected and dead trees than under healthy trees. Accordingly, we also found a significant relationship between the seasonal means of R_s and those of precipitation under affected ($\rho = 0.81$, $P < 0.05$) and dead ($\rho = 0.83$, $P < 0.05$) trees but not under healthy trees ($\rho = 0.69$, $P = 0.07$).

3.3. Tree decline changes the relative importance of the main drivers of soil respiration

The multimodel inference approach revealed that canopy diameter (surrogate of tree decline status) and soil total N were the most important predictors for the two-year average values of R_s considering all decline stages together (Fig. 3, Table S3). Total N was also the most important predictor of R_s considering healthy trees separately (Fig. 3, Table S3), but it was not a good predictor for the R_s under affected and dead trees, which shared labile C as one of their most important predictors. Bulk density and T_{soil} were the second and third most important predictors of R_s under affected trees, whereas, under dead trees, T_{soil} and SWC occupied the first and the third position, respectively, explaining, along with labile C, up to 93% of the variance of R_s (Table S3).

4. Discussion

4.1. Interacting effects of year, season, and tree decline on soil microclimate and R_s

The 16% higher annual precipitation in *year 2* compared to that in *year 1* led to higher SWC and R_s (14%) annual means (Table 1). These differences in R_s between years were likely driven by not only the differences in the amount but also in the timing of precipitation between years (Maier et al., 2011). The rainfall events at the end of the summer and the beginning of the fall of 2014 (Fig. 1) are typical of these ecosystems and coincide with optimal temperature and nutrient availability conditions after an extensive drought period. These conditions trigger an

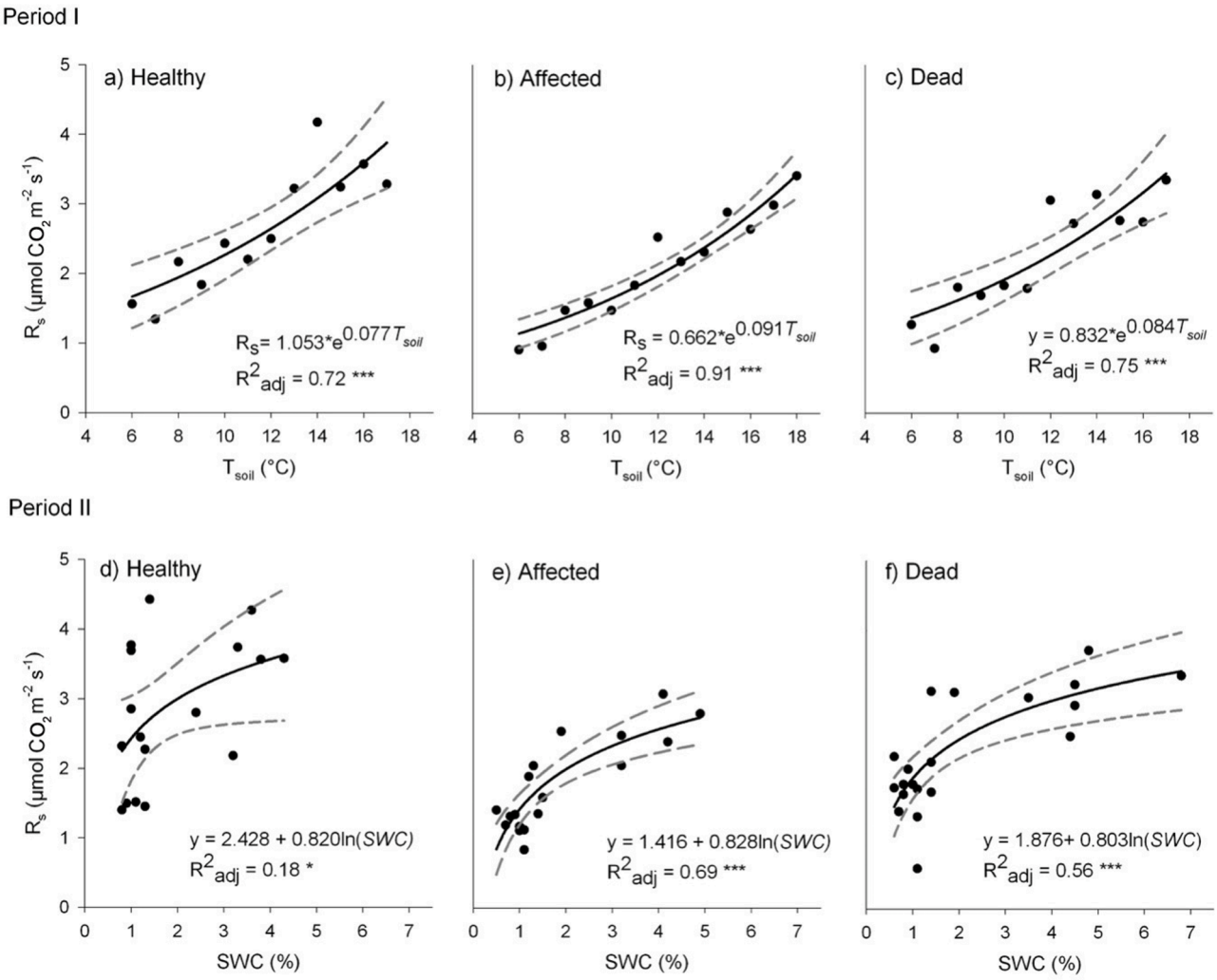

Fig. 2. Relationship between soil respiration (R_s) and soil temperature (top figures, Period I) and SWC (bottom figures, Period II) for healthy (a, d), affected (b, e), and dead (c, f) trees, respectively, using averaged values for each temperature degree. The black solid line and the dashed gray lines represent the fitted regression and the 95% confidence interval, respectively. The adjusted R^2 (R^2_{adj}) values were used as a measure of the goodness-of-fit of the models. Significant relationships are denoted by *** ($P < 0.001$) and * ($P < 0.05$). T_{soil} = soil temperature; SWC= soil water content.

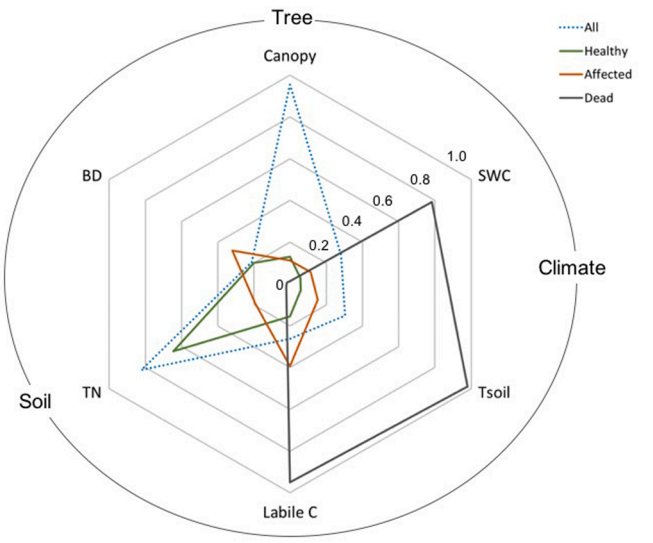

Fig. 3. Relative importance of tree (i.e. Canopy) and soil microclimatic (i.e. soil water content and soil temperature) and physicochemical (i.e. Labile C, total N, bulk density) variables as predictors of two-year average values of R_s under healthy, affected, and dead trees separately and together in a Mediterranean holm oak forest from the central part of the Iberian Peninsula. Canopy, canopy diameter; SWC, soil water content; T_{soil}, soil temperature; Labile C, total carbon in the magnetic fraction; TN, total N; BD, bulk density.

intense peak in microbial activity, a phenomenon known as the 'Birch effect' (Birch, 1958), as well as high plant activity (Rousk and C. Brangarí, 2022). Contrary, *Year 1* showed the highest soil moisture conditions in winter, after a long period of chained rainfall events that do not have a comparable effect, and when biotic (plant and microbial) activity is normally stable and low due to the cold temperature (Maier et al., 2011). Further, the higher differences in R_s between years observed under healthy (22%) than under affected (5%) and dead (16%) trees (Table 1) suggest that tree decline decreases the positive response of R_s to increases in annual precipitation and drying-rewetting cycles. These field observations, based on only two years, are supported by the highest positive response of R_H to induced drying-rewetting cycles in soils collected under healthy trees at the same site and incubated in the laboratory in a previous study (Rodríguez et al., 2019). Investigating the microbial responses to drying-rewetting cycles has been a fundamental challenge in soil science for nearly a century (Rousk and C. Brangarí, 2022). Microbial ecologists have reached a consensus that drying-rewetting cycles play a crucial role in the soil-atmosphere C exchange process (Rey et al., 2021; Rousk and C. Brangarí, 2022). However, this consensus is based on limited experimental units and laboratory settings that often exclude plants, while the impact of rewetting dry soil on C cycling at the ecosystem level and its interaction with other environmental changes remains largely understudied (Rousk and C. Brangarí, 2022). Our findings contribute new perspectives to this important topic and underscore the necessity for regular monitoring during drying-rewetting episodes to capture field soil CO_2 emission spikes and for taking into account tree health and precipitation distribution in ecosystem C balances and climate-change models.

As hypothesized, our study showed that tree decline influences soil microclimatic conditions, particularly SWC, and R_s, but the magnitude of these effects would vary among seasons and years due to contrasting biotic activity and precipitation conditions (i.e. amount and distribution), respectively. The trend toward increased maximums of T_{soil} during the whole studied period and the decrease in the values for fall 2014 with defoliation degree (Table 2) reflects the important role of healthy canopies in protecting the soil from large changes in air temperature (Lozano-Parra et al., 2018). Supporting the higher SWC values under dead than under living trees observed by Curiel Yuste et al. (2019) in mountain temperate conifer forests from Eastern Romanian Carpathians, we found overall higher values of SWC under dead than under healthy trees, and intermediate values under affected trees (Table 1). This positive effect could be the result of enhanced accumulation of soil organic matter (i.e. litterfall inputs from both above- and belowground) but also reduced absorption and capture of water from roots and canopies, respectively (Anderegg et al., 2012; Wang et al., 2012). Although we did not find a similar overall effect of tree decline on R_s, we did find significant interactions between tree decline and climatic variability (annual and seasonal), with higher values of R_s under healthy than under affected trees, particularly in *year 2* (i.e. the most humid year) and in all seasons except in spring, and intermediate values under dead trees. Besides altering soil abiotic conditions, drought-induced tree decline might limit the supply of photosynthates to the radical organs and exudates and dead organic matter to soil microbial communities (e.g. Högberg et al., 2001; Barba et al., 2016). This disruption of the belowground C allocation is known to decrease R_A and R_H (Högberg et al., 2001; Nave et al., 2011), thus explaining the decrease in R_s under affected trees. However, in the case of dead trees, increases in litterfall, resource (e.g., carbon, nutrients, and light) availability, and other processes as a result of canopy losses (e.g., photodegradation and exposure to small rainfall pulses and dew; Rey et al., 2011; Gilkman et al., 2018; Wang et al., 2012) might have enhanced R_H and compensated, at least partially, the assumed decrease in R_A (e.g., Curiel Yuste et al., 2019). Indeed, Moore et al. (2013) found a tree mortality-driven initial decline in soil respiration of subalpine forest sandy soils with a thin organic horizon from the Western United States, a partial recovery after about 5–6 years associated with increased incorporation of leaf litter C into soil organic matter, and a further decline in years 8–10. Although we do not know exactly when our holm oak trees died, the fact that most of the dead trees were still standing when we performed the study indicates that it occurred a short time before our sampling (< 10 years). Therefore, it is likely that our results might correspond to the temporary recovery of soil respiration under dead trees observed by Moore et al. (2013). Also, expressing R_s on a C basis (i.e. per unit of soil organic C) allowed us to account for the influence of different amounts of soil organic C determining the observed differences among decline stages and, thus, somehow understand how mineralizable (i.e. labile) that C is and/or how important the autotrophic component is for the R_s. The fact that we found the same pattern but without statistically significant differences among decline stages for any of the two years when expressing R_s on a soil C basis (Table 1) stresses the important role of soil C content and R_H, and to a lesser extent of soil C lability and/or R_A, as drivers of that response. In a previous study on the same site, Rodríguez et al. (2017) found that while potential R_H was up to 66% lower under affected than under healthy trees, dead trees showed similar values of R_H to those of healthy trees. Thus, although these previous results do not support the hypothesis of higher R_H under dead than under healthy trees, they do suggest a potential recovery of R_H after tree death. Although we did not analyze the different components of R_s separately, and the R_H values from Rodríguez et al. (2017) do not take into account all the climatic variability of our two-year study, all above suggest that the heterotrophic component could have a key role in the observed response of R_s to tree decline in this Mediterranean woodland.

The apparent lack of effect of forest die-off on soil C and nutrient cycling during spring could be largely explained by the herbaceous colonization under declining trees (Rodríguez et al., 2017) and the peak activity of herbaceous roots during this season, which may have helped offset the negative effect of tree decline over the tree and soil microbial activity (Avila et al., 2016; Rodríguez et al., 2019; Tang and Baldocchi, 2005). On the other hand, whereas we did not find differences in winter T_{soil} and summer SWC among decline stages, we did find them in R_s in both winters and summers (Table 2), suggesting a high resilience of the R_A component to unfavorable climatic conditions in healthy but not in declining trees. In any case, our study shows that the soil effects of tree decline are detectable before tree death. Further, our results suggest

that, as mortality increases in this type of woodlands, and provided that conditions for microbial functioning are met, they could still emit a significant amount of CO_2 while likely fixing much less C from the atmosphere than healthy woodlands. This situation could lead, at least in the short- (i.e. years) to medium-term (i.e. decades), to a swift in the role of these forests from sinks to sources of C (Baldocchi et al., 2004; Nave et al., 2011; Xiong et al., 2011). The strong negative effects of forest die-off on both soil C content and lability observed in this system by Rodríguez et al. (2020) support this hypothesis. All these results highlight the need to consider both the spatial (i.e. different declining stages) and climatic (seasonal and annual) variability, two components still scarcely explored together, when trying to fully understand the complex effects of tree decline on soil biogeochemical conditions and functioning (Avila et al., 2016).

4.2. Effect of tree decline on the relationship of R_s with soil microclimatic conditions

As expected (e.g., Rey et al., 2011; Barba et al., 2016), R_s was better explained by T_{soil} up to a determined threshold (Period I), which corresponded with still optimal T_{soil} (~17 °C) but low SWC (< 7%) conditions (Figs. 2 and S1). Thus, once SWC reached limiting values, R_s was no longer better explained by T_{soil} but by SWC (Period II) (Fig. 2), highlighting the key role of water availability in the functioning of Mediterranean ecosystems (Reichstein et al., 2002; Rey et al., 2011, 2002). The basal respiration values obtained from the exponential relationships between R_s and T_{soil} followed the pattern of potential microbial respiration found by Rodríguez et al. (2017) and supported the lower respiration activity found under affected than under healthy trees in our study. Interestingly, the higher Q_{10} values and variances of R_s explained by T_{soil} and SWC under declining than under healthy trees, along with the significant correlations found between the seasonal means of R_s and those of precipitation only under declining trees might suggest that the control of R_s by T_{soil} and SWC increases with tree decline. As autotrophic and heterotrophic respirations at the stand level are mainly controlled by plants and soil microclimate, respectively (Chen et al., 2019; Högberg et al., 2001; Matteucci et al., 2015), our results might indicate an increase in the relative contribution of the heterotrophic respiration under tree decline. In any case, these results stress the capacity of tree decline to sharply modulate the relationship of R_s with soil microclimatic variables.

4.3. Main drivers of R_s at the stand scale

Our results confirmed our third hypothesis about tree decline changing the relative importance of the different drivers of R_s. The relative importance of SWC and T_{soil} increased against that of plant variables from considering the whole decline gradient to considering each stage separately in increasing decline (from healthy to dead trees). Canopy diameter (a good proxy of tree decline; see methods section) was the most important predictor of R_s (Fig. 3, Table S3), indicating that, at the stand level, healthier trees with larger canopies support higher R_s rates. These results highlight both the important role of tree decline (i.e. health status) as a driver of the ecosystem functioning and the important contribution of the autotrophic component to R_s in our ecosystem. Along with canopy diameter, total N was also a very important predictor of R_s, and the most important predictor under healthy trees, supporting the notion of N as a key nutrient for these ecosystems' functioning (Högberg et al., 2001). Furthermore, the observed negative correlation between canopy diameter and the C:N ratio (Figure S2) supports the previously observed negative effect of forest die-off on soil organic matter quality and N availability (Rodríguez et al., 2020, 2017). Altogether, these results warn about likely positive feedback between forest die-off and N limitation (Gessler et al., 2016), with important implications for the ecosystem C and N balance.

Tree defoliation triggers a cascade effect on plant understory and soil microbial communities with important implications for ecosystem C and N budgets, including a decrease in soil organic matter lability (Rodríguez et al., 2020, 2017), which could largely affect R_H (Rodríguez et al., 2019; Rui et al., 2016). As discussed above, C:N ratio increased as canopy diameter decreased, supporting the negative effect of tree defoliation and mortality on soil organic matter quality. Accordingly, the best models for both affected and dead trees included labile C as one of the most important R_s predictors (Fig. 3, Table S3). Bulk density and T_{soil} were the second and third most important predictors for R_s under affected trees, whereas the best model of R_s under dead trees included T_{soil} and SWC as the most important predictors. Bulk density is widely recognized to be negatively related to soil organic matter content (Périé and Ouimet, 2008) and roots mass (Daddow and Warrington, 1983), which are among the main controls of R_H and R_A, respectively. These results would agree with the above-discussed parallel decrease in R_A and R_H under affected trees and almost complete substitution of R_s for R_H under dead trees. Finally, whereas the best models for healthy and affected trees never surpassed 50% of the variance explained, the best model for dead trees reached 93% of the variance explained with just bulk density and both soil microclimatic variables as predictors. This result might suggest a simplification of the control of the soil respiration process under tree decline, going from depending on many physiological, phenological, and environmental factors to largely depending on just a few of them, which could jeopardize its resilience to global change drivers, including climate change (Hong et al., 2022).

5. Conclusions

Our study adds robust and novel in situ evidence of interacting effects between climatic variability and drought-induced tree decline on the spatial-temporal variability of R_s in Mediterranean holm-oak forests. Our findings indicate that the response of soil respiration to variations in precipitation is higher under healthy trees than under declining trees, emphasizing the crucial role of tree health as a modulator of soil respiration in response to soil moisture conditions. Our study also demonstrates that tree decline significantly impacts soil moisture and R_s in these Mediterranean forests, with the magnitude of this effect varying based on factors such as the stage of decline (i.e. affected or dead), the year, and the season. Further, our study demonstrates that tree decline alters the relative importance of different drivers of soil respiration, with soil water content and temperature becoming increasingly important as the degree of defoliation increases. Finally, our research suggests a potential positive feedback between forest die-off and N limitation, as well as a simplification of the soil respiration process with tree decline. Altogether, our results point towards still understudied negative impacts of drought-induced tree decline on soil C content and cycling, particularly under anticipated climate change scenarios with dryer and more intense precipitation regimes. Therefore, further studies investigating the joint effects of drought-induced forest die-off and climatic variability on soil respiration and its main components at various temporal and spatial scales are needed to fully understand the fate of this important ecosystem process.

Declaration of Competing Interest

The authors declare that they have no known competing financial interests or personal relationships that could have appeared to influence the work reported in this paper.

Data availability

Data will be made available on request.

Acknowledgments

This research was supported by the Spanish National Research Council (CSIC) in the JAE-doc modality co-financed by the European Social Fund (ESF), the ATLANTIS (PID2020–113244GB-C21) projects funded by the Spanish Government, the Basque Government through the BERC 2022–2025 program, and the Spanish Ministry of Science and Innovation through the BC3 María de Maeztu excellence accreditation (MDM-2017–0714). J.D. and A.R. acknowledge support from the FCT (2020.03670.CEECIND and SFRH/BDP/108913/2015, respectively), as well as from the MCTES, FSE, UE, and the CFE (UIDB/04004/2021) research unit financed by FCT/MCTES through national funds (PIDDAC). The authors are grateful to all the people who at some point helped with fieldwork, particularly David López, as well as to the editor and three reviewers. Also, special thanks to Maria José Fernández Alonso and Luis Maria Carrascal for their advice on statistics.

Supplementary materials

Supplementary material associated with this article can be found, in the online version, at doi:10.1016/j.agrformet.2023.109398.

References

Anderegg, W.R.L., Anderegg, L.D.L., Sherman, C., Karp, D.S., 2012. Effects of widespread drought-induced aspen mortality on understory plants. Conserv. Biol. 26, 1082–1090. https://doi.org/10.1111/j.1523-1739.2012.01913.x.

Avila, J.M., Gallardo, A., Gómez-Aparicio, L., 2019. Pathogen-induced tree mortality interacts with predicted climate change to alter soil respiration and nutrient availability in Mediterranean systems. Biogeochemistry 142, 53–71. https://doi.org/10.1007/s10533-018-0521-3.

Avila, J.M., Gallardo, A., Ibáñez, B., Gómez-Aparicio, L., 2016. Quercus suber dieback alters soil respiration and nutrient availability in Mediterranean forests. J. Ecol. 104, 1441–1452. https://doi.org/10.1111/1365-2745.12618.

Baldocchi, D.D., Xu, L., Kiang, N., 2004. How plant functional-type, weather, seasonal drought, and soil physical properties alter water and energy fluxes of an oak–grass savanna and an annual grassland. Agric. For. Meteorol. 123, 13–39. https://doi.org/10.1016/j.agrformet.2003.11.006.

Barba, J., Curiel Yuste, J., Martínez-Vilalta, J., Lloret, F., 2013. Drought-induced tree species replacement is reflected in the spatial variability of soil respiration in a mixed Mediterranean forest. For. Ecol. Manage. 306, 79–87. https://doi.org/10.1016/j.foreco.2013.06.025.

Barba, J., Curiel Yuste, J., Poyatos, R., Janssens, I.A., Lloret, F., 2016. Strong resilience of soil respiration components to drought-induced die-off resulting in forest secondary succession. Oecologia 1–15. https://doi.org/10.1007/s00442-016-3567-8.

Birch, H.F., 1958. The effect of soil drying on humus decomposition and nitrogen availability. Plant Soil 10, 9–31. https://doi.org/10.1007/BF01343734.

Bretz, F., Hothorn, T., Westfall, P., 2011. Multiple Comparisons Using R. CRC Press.

Burnham, K.P., Anderson, D.R., 2010. Model Selection and Multimodel Inference: A Practical Information-Theoretic Approach, 2nd edition. Springer, New York, USA.

Carnicer, J., Coll, M., Ninyerola, M., Pons, X., Sánchez, G., Peñuelas, J., 2011. Widespread crown condition decline, food web disruption, and amplified tree mortality with increased climate change-type drought. Proc. Natl Acad. Sci. 108, 1474–1478. https://doi.org/10.1073/pnas.1010070108.

Chen, Z., Xu, Y., Castellano, M.J., Fontaine, S., Wang, W., Ding, W., 2019. Soil respiration components and their temperature sensitivity under chemical fertilizer and compost application: the role of nitrogen supply and compost substrate quality. J. Geophys. Res. 124, 556–571. https://doi.org/10.1029/2018JG004771.

Chiti, T., Certini, G., Marzaioli, F., D'Acqui, L.P., Forte, C., Castaldi, S., Valentini, R., 2019. Composition and turnover time of organic matter in soil fractions with different magnetic susceptibility. Geoderma 349, 88–96. https://doi.org/10.1016/j.geoderma.2019.04.042.

Curiel Yuste, J., Baldocchi, D.D., Gershenson, A., Goldstein, A., Misson, L., Wong, S., 2007. Microbial soil respiration and its dependency on carbon inputs, soil temperature and moisture. Glob. Chang. Biol. 13, 2018–2035. https://doi.org/10.1111/j.1365-2486.2007.01415.x.

Curiel Yuste, J., Flores-Rentería, D., García-Angulo, D., Hereş, A.-M., Bragă, C., Petritan, A.-M., Petritan, I.C., 2019. Cascading effects associated with climate-change-induced conifer mortality in mountain temperate forests result in hot-spots of soil CO2 emissions. Soil Biol. Biochem. 133, 50–59. https://doi.org/10.1016/j.soilbio.2019.02.017.

Daddow, R.L., Warrington, G., 1983. Growth-limiting Soil Bulk Densities As Influenced By Soil texture. Watershed Systems Development Group. USDA Forest Service.

Edburg, S., Hicke, J., Brooks, P., Pendall, E., Ewars, B., Norton, U., Gochis, D., Guttman, E., Meddens, A., 2012. Cascading impacts of bark beetle-caused tree mortality on coupled biogeophysical and biogeochemical processes. Front. Ecol. Environ. 10, 416–424. https://doi.org/10.1890/110173.

Gallardo, A., Covelo, F., Morillas, L., Delgado, M., 2009. Ciclos de nutrientes y procesos edáficos en los ecosistemas terrestres: especificidades del caso mediterráneo y sus implicaciones para las relaciones suelo-planta. Revista Ecosistemas 18. https://doi.org/10.7818/re.2014.18-2.00.

García-Angulo, D., Hereş, A.-M., Fernández-López, M., Flores, O., Sanz, M.J., Rey, A., Valladares, F., Curiel Yuste, J., 2020. Holm oak decline and mortality exacerbates drought effects on soil biogeochemical cycling and soil microbial communities across a climactic gradient. Soil Biol. Biochem. 107921 https://doi.org/10.1016/j.soilbio.2020.107921.

Gessler, A., Schaub, M., McDowell, N.G., 2016. The role of nutrients in drought-induced tree mortality and recovery. New Phytol. https://doi.org/10.1111/nph.14340 n/a-n/a.

Guerra, C.A., Berdugo, M., Eldridge, D.J., Eisenhauer, N., Singh, B.K., Cui, H., Abades, S., Alfaro, F.D., Bamigboye, A.R., Bastida, F., Blanco-Pastor, J.L., de los Ríos, A., Durán, J., Grebenc, T., Illán, J.G., Liu, Y.-.R., Makhalanyane, T.P., Mamet, S., Molina-Montenegro, M.A., Moreno, J.L., Mukherjee, A., Nahberger, T.U., Peñaloza-Bojacá, G.F., Plaza, C., Picó, S., Verma, J.P., Rey, A., Rodríguez, A., Tedersoo, L., Teixido, A.L., Torres-Díaz, C., Trivedi, P., Wang, Juntao, Wang, L., Wang, Jianyong, Zaady, E., Zhou, X., Zhou, X.-.Q., Delgado-Baquerizo, M., 2022. Global hotspots for soil nature conservation. Nature 610, 693–698. https://doi.org/10.1038/s41586-022-05292-x.

Hegyi, F., 1974. A simulation model for managing jack-pine stands. Growth Models for Tree and Stand Simulation. Royal College of Forestry,, Stockholm, Sweden, pp. 74–90.

Högberg, P., Nordgren, A., Buchmann, N., Taylor, A.F.S., Ekblad, A., Högberg, M.N., Nyberg, G., Ottosson-Löfvenius, M., Read, D.J., 2001. Large-scale forest girdling shows that current photosynthesis drives soil respiration. Nature 411, 789–792. https://doi.org/10.1038/35081058.

Hong, P., Schmid, B., De Laender, F., Eisenhauer, N., Zhang, X., Chen, H., Craven, D., De Boeck, H.J., Hautier, Y., Petchey, O.L., Reich, P.B., Steudel, B., Striebel, M., Thakur, M.P., Wang, S., 2022. Biodiversity promotes ecosystem functioning despite environmental change. Ecol. Lett. 25, 555–569. https://doi.org/10.1111/ele.13936.

IPCC, 2021. Climate Change 2021: The Physical Science Basis. Contribution of Working Group I to the Sixth Assessment Report of the Intergovernmental Panel On Climate Change. Cambridge University Press ed.

Liu, Y., Liu, S., Wan, S., Wang, J., Luan, J., Wang, H., 2016. Differential responses of soil respiration to soil warming and experimental throughfall reduction in a transitional oak forest in central China. Agric. For. Meteorol. 226 (227), 186–198. https://doi.org/10.1016/j.agrformet.2016.06.003.

Lloret, F., Siscart, D., Dalmases, C., 2004. Canopy recovery after drought dieback in holm-oak Mediterranean forests of Catalonia (NE Spain). Glob Chang Biol 10, 2092–2099. https://doi.org/10.1111/j.1365-2486.2004.00870.x.

Lozano-Parra, J., Pulido, M., Lozano-Fondón, C., Schnabel, S., 2018. How do soil moisture and vegetation covers influence soil temperature in drylands of mediterranean regions? Water (Basel) 10, 1747. https://doi.org/10.3390/w10121747.

Maier, M., Schack-Kirchner, H., Hildebrand, E.E., Schindler, D., 2011. Soil CO2 efflux vs. soil respiration: implications for flux models. Agric. For. Meteorol. 151, 1723–1730. https://doi.org/10.1016/j.agrformet.2011.07.006.

Matteucci, M., Gruening, C., Goded Ballarin, I., Seufert, G., Cescatti, A., 2015. Components, drivers and temporal dynamics of ecosystem respiration in a Mediterranean pine forest. Soil Biol. Biochem. 88, 224–235. https://doi.org/10.1016/j.soilbio.2015.05.017.

Moore, D.J.P., Trahan, N.A., Wilkes, P., Quaife, T., Stephens, B.B., Elder, K., Desai, A.R., Negron, J., Monson, R.K., 2013. Persistent reduced ecosystem respiration after insect disturbance in high elevation forests. Ecol. Lett. 16, 731–737. https://doi.org/10.1111/ele.12097.

Nave, L.E., Gough, C.M., Maurer, K.D., Bohrer, G., Hardiman, B.S., Le Moine, J., Munoz, A.B., Nadelhoffer, K.J., Sparks, J.P., Strahm, B.D., Vogel, C.S., Curtis, P.S., 2011. Disturbance and the resilience of coupled carbon and nitrogen cycling in a north temperate forest. J. Geophys. Res. 116, G04016. https://doi.org/10.1029/2011JG001758.

Ninyerola, M., Pons, X., Roure, J., 2005. Atlas Climático Digital De La Península Ibérica. Metodología y Aplicaciones En Bioclimatología y Geobotánica. Universidad Autónoma de Barcelona, Barcelona, Spain.

Périé, C., Ouimet, R., 2008. Organic carbon, organic matter and bulk density relationships in boreal forest soils. Can. J. Soil. Sci. 88, 315–325. https://doi.org/10.4141/CJSS06008.

Pinheiro, J., Bates, D., DebRoy, S., Sarkar, D., R Core Team, 2020. nlme: linear and nonlinear mixed effects models. R package version 3.1–148.

Core Team, R., 2017. R: A language and Environment For Statistical Computing. R Foundation for Statistical Computing, Vienna, Austria.

Raich, J.W., Schlesinger, W.H., 1992. The global carbon dioxide flux in soil respiration and its relationship to vegetation and climate. Tellus B 44, 81–99. https://doi.org/10.1034/j.1600-0889.1992.t01-1-00001.x.

Rangel, T.F., Diniz-Filho, J.A.F., Bini, L.M., 2010. SAM: a comprehensive application for spatial analysis in macroecology. Ecography 33, 46–50. https://doi.org/10.1111/j.1600-0587.2009.06299.x.

Reichstein, M., Bahn, M., Ciais, P., Frank, D., Mahecha, M.D., Seneviratne, S.I., Zscheischler, J., Beer, C., Buchmann, N., Frank, D.C., Papale, D., Rammig, A., Smith, P., Thonicke, K., van der Velde, M., Vicca, S., Walz, A., Wattenbach, M., 2013. Climate extremes and the carbon cycle. Nature 500, 287–295. https://doi.org/10.1038/nature12350.

Reichstein, M., Tenhunen, J.D., Roupsard, O., Ourcival, J., Rambal, S., Miglietta, F., Peressotti, A., Pecchiari, M., Tirone, G., Valentini, R., 2002. Severe drought effects on ecosystem CO2 and H2O fluxes at three Mediterranean evergreen sites: revision of current hypotheses? Glob. Chang. Biol. 8, 999–1017. https://doi.org/10.1046/j.1365-2486.2002.00530.x.

Rey, A., Carrascal, L.M., Báez, C.G.-G., Raimundo, J., Oyonarte, C., Pegoraro, E., 2021. Impact of climate and land degradation on soil carbon fluxes in dry semiarid grasslands in SE Spain. Plant Soil 461, 323–339. https://doi.org/10.1007/s11104-021-04842-y.

Rey, A., Oyonarte, C., Morán-López, T., Raimundo, J., Pegoraro, E., 2017. Changes in soil moisture predict soil carbon losses upon rewetting in a perennial semiarid steppe in SE Spain. Geoderma 287, 135–146. https://doi.org/10.1016/j.geoderma.2016.06.025.

Rey, A., Pegoraro, E., Oyonarte, C., Were, A., Escribano, P., Raimundo, J., 2011. Impact of land degradation on soil respiration in a steppe (Stipa tenacissima L.) semi-arid ecosystem in the SE of Spain. Soil Biol. Biochem. 43, 393–403. https://doi.org/10.1016/j.soilbio.2010.11.007.

Rey, A., Pegoraro, E., Tedeschi, V., De Parri, I., Jarvis, P.G., Valentini, R., 2002. Annual variation in soil respiration and its components in a coppice oak forest in Central Italy. Glob. Chang. Biol. 8, 851–866. https://doi.org/10.1046/j.1365-2486.2002.00521.x.

Rodríguez, A., Chiti, T., Rey, A., Durán, J., 2020. Forest die-off reduces soil C and N content and increases C stability in a Mediterranean woodland. Geoderma 359, 113990. https://doi.org/10.1016/j.geoderma.2019.113990.

Rodríguez, A., Durán, J., Rey, A., Boudouris, I., Valladares, F., Gallardo, A., Yuste, J.C., 2019. Interactive effects of forest die-off and drying-rewetting cycles on C and N mineralization. Geoderma 333, 81–89. https://doi.org/10.1016/j.geoderma.2018.07.003.

Rodríguez, A., Yuste, J.C., Rey, A., Durán, J., García-Camacho, R., Gallardo, A., Valladares, F., 2017. Holm oak decline triggers changes in plant succession and microbial communities, with implications for ecosystem C and N cycling. Plant Soil 414, 247–263. https://doi.org/10.1007/s11104-016-3118-4.

Rousk, J., C. Brangarí, A., 2022. Do the respiration pulses induced by drying–rewetting matter for the soil–atmosphere carbon balance? Glob. Chang. Biol. 28, 3486–3488. https://doi.org/10.1111/gcb.16163.

Rui, Y., Murphy, D.V., Wang, X., Hoyle, F.C., 2016. Microbial respiration, but not biomass, responded linearly to increasing light fraction organic matter input: consequences for carbon sequestration. Sci. Rep. 6, 35496. https://doi.org/10.1038/srep35496.

Schlesinger, W.H., Andrews, J.A., 2000. Soil respiration and the global carbon cycle. Biogeochemistry 48, 7–20. https://doi.org/10.1023/A:1006247623877.

Schlesinger, W.H., Dietze, M.C., Jackson, R.B., Phillips, R.P., Rhoades, C.C., Rustad, L.E., Vose, J.M., 2016. Forest biogeochemistry in response to drought. Glob. Chang. Biol. 22, 2318–2328. https://doi.org/10.1111/gcb.13105.

Taiyun, W., Simko, V., 2017. R package "corrplot": visualization of a correlation matrix version 0.84 from CRAN.

Tang, J., Baldocchi, D.D., 2005. Spatial–temporal variation in soil respiration in an oak–grass savanna ecosystem in California and its partitioning into autotrophic and heterotrophic components. Biogeochemistry 73, 183–207. https://doi.org/10.1007/s10533-004-5889-6.

Wang, Q., He, N., Liu, Y., Li, M., Xu, li, 2016. Strong pulse effects of precipitation events on soil microbial respiration in temperate forests. Geoderma 275, 67–73. https://doi.org/10.1016/j.geoderma.2016.04.016.

Wang, W., Peng, C., Kneeshaw, D.D., Larocque, G.R., Luo, Z., 2012. Drought-induced tree mortality: ecological consequences, causes, and modeling. Environ. Rev. 20, 109–121.

Warner, D.L., Bond-Lamberty, B., Jian, J., Stell, E., Vargas, R., 2019. Spatial predictions and associated uncertainty of annual soil respiration at the global scale. Global Biogeochem. Cycles 33, 1733–1745. https://doi.org/10.1029/2019GB006264.

Xiong, Y., D'Atri, J.J., Fu, S., Xia, H., Seastedt, T.R., 2011. Rapid soil organic matter loss from forest dieback in a subalpine coniferous ecosystem. Soil Biol. Biochem. 43, 2450–2456. https://doi.org/10.1016/j.soilbio.2011.08.013.

Zhao, C., Miao, Y., Yu, C., Zhu, L., Wang, F., Jiang, L., Hui, D., Wan, S., 2016. Soil microbial community composition and respiration along an experimental precipitation gradient in a semiarid steppe. Sci. Rep. 6, 24317. https://doi.org/10.1038/srep24317.